

## Identify the Optimal Sensor Location: Analysis of Flue Gas Behavior in Stack by Using CFD Simulation

Suhazrin Najihah Suaimi<sup>1</sup>, Mohd Azahari Razali<sup>1\*</sup>, Iman Fitri Ismail<sup>1</sup>,  
Norfakhira Mohd Nor<sup>1</sup>, Masataro Suzuki<sup>2</sup>, Mohd Azni Md Kassim<sup>3</sup>

<sup>1</sup> Faculty of Mechanical and Manufacturing Engineering

Universiti Tun Hussein Onn Malaysia, 86400 Parit Raja, Batu Pahat, Johor, MALAYSIA

<sup>2</sup> Department of System Safety Engineering,

Institute of GIGAKU, Nagaoka University of Technology, Nagaoka, Niigata, JAPAN

<sup>3</sup> Tuah Consult Sdn. Bhd,

T4-2-2, Tower 4, Level 2, Maju Link, Jalan Lingkaran Tengah II (MRR2), 57100 Bandar Tasik Selatan, Kuala Lumpur, MALAYSIA

\*Corresponding Author: [azahari@uthm.edu.my](mailto:azahari@uthm.edu.my)

DOI: <https://doi.org/10.30880/rpmme.2025.06.02.029>

### Article Info

Received: 31 July 2025

Accepted: 31 October 2025

Available online: 10 December 2025

### Keywords

CFD, Flue Gas Monitoring Sensor  
Placement, Emission Analysis,  
Industrial Stack

### Abstract

Industrial flue gas emission consists of harmful substance such as carbon monoxide (CO), carbon dioxide (CO<sub>2</sub>), nitrogen oxides (NO<sub>x</sub>), sulfur dioxide (SO<sub>2</sub>), which contribute to air pollution, climate change, and health risks. Effective emission monitoring is essential to reduce environmental impact and comply with air quality regulations. However, the accuracy of in-situ gas sensors largely depends on proper placement within the exhaust stack, as poor positioning in turbulent or unstable flow regions can result in inaccurate readings. This study aims to analyze flue gas flow behavior within an L-shaped industrial exhaust stack and determine the optimal sensor placement using Computational Fluid Dynamic (CFD) simulation. The geometry was created in SolidWorks and imported into ANSYS Fluent 2024 R1 for steady state analysis using the standard k-epsilon turbulence model. Key flow parameters such as velocity, pressure, and gas interaction with sensor geometry were examined. The stack consists of a 4-meter horizontal section, a 12-meter vertical section, and a 2-meter diameter. Four sensor locations 2 m, 4 m, 6 m, and 8 m from the outlet were tested to evaluate flow stability and suitability for sensor installation. Simulation results showed that the sensor location at 10 meters from the bend which is 2 meters before the outlet offered the most stable flow conditions, with an average velocity of 10.75 m/s and a pressure difference of only 59.5 Pa across the sensor. This minimal pressure drop indicates low flow disturbance caused by the sensor, helping maintain continuous and reliable contact between the flue gas and the sensor surface. These favorable flow characteristics support the accuracy of gas detection and confirm this location as optimal for in-situ sensor deployment. Overall, the findings demonstrate the effectiveness of CFD in guiding sensor placement strategies for enhanced emission monitoring in industrial stack systems.

## 1. Introduction

Industrial activities involving combustion processes are a significant source of flue gas emissions containing pollutants such as CO<sub>2</sub>, NO<sub>x</sub>, and SO<sub>2</sub>, which contribute to environmental degradation and health issues [1]. In Malaysia, industrial sectors such as oil and gas, manufacturing, and power generation are major contributors to flue gas emissions, underscoring the importance of continuous monitoring strategies. According to Elseoud et al., [2], high emissions levels are linked to urban air quality deterioration, necessitating effective control measures. To address this, in-situ sensor technology has been widely adopted for real time emission monitoring. Nawawi et al. [3] states that it is essential for industries utilizing flue gas systems to monitor these emissions closely to comply with the Environmental Quality (Clean Air) Regulations 2014, which establish strict standards for air pollutants [4]

Previous studies by Sarwar et al. [5] have highlighted the importance of understanding flow behavior in exhaust systems to improve sensor efficiency and monitoring accuracy. Johnson et al [6] compared several methods for measuring gas velocity in stacks and concluded that stable flow zones produce more consistent sensor readings. Shen et al. [7] emphasized that flow uniformity and temperature gradients significantly influence sensor performance. In another study, Guo et al., [8], designed a multi-laser hybrid absorption sensor to measure N<sub>2</sub>, NO, and temperature in flue gas, showing the significance of correct positioning for accuracy. These findings support the current research, which applies CFD simulation to determine ideal sensor locations heavily depends on sensor placement, which directly influences measurement accuracy. Furthermore, Anderson et al. and Farid & Solav [9][1] highlight the importance of environmental sensors in monitoring pollution. Nevertheless, the placement of these sensors presents a challenge, as suboptimal positioning can lead to inaccurate data, complicating emission positioning can lead to inaccurate data, complicating emission evaluations [2]

Computational Fluid Dynamic (CFD) has emerged as a powerful tool for analyzing internal flow characteristics and optimizing sensor positions. G et al. [3] emphasized the role of modeling tools like CFD in predicting and mitigating emissions from industrial systems. This study aims to analyze the flue gas behavior in an L-shaped exhaust stack to determine optimal sensor placement based on flow stability, pressure distribution, and interaction with sensor geometry. By focusing on realistic conditions and using advanced simulation software (ANSYS Fluent), the study contributes to more reliable emission measurement practices. The findings are also aligned with global sustainability goals such as SDG 13 (Climate Action), by supporting pollution reduction and clean air initiatives.

## 2. Methodology

The methodology describes how to achieve the objective of the study focusing on applying Computational Fluid Dynamics (CFD) to analyse flue gas emissions. This study measure parameters such as temperature, velocity, and pollutant concentrations to determine optimal sensor placement for accurate monitoring. The process involves creating virtual models of the flue gas system, generating mesh, and running simulations in ANSYS Fluent to study gas flow and pollutant behavior. The results help ensure better emissions control and meet environmental standards.

### 2.1 Geometry Modeling

The flue gas stack was designed in SolidWorks with an L-shaped configuration consisting of a 4 m horizontal pipe connected to a 12 m vertical outlet pipe as shown in Fig. 1. The internal diameter of the pipe is 2 m. Four sensor locations were defined at 4 m, 6m, 8 m, and 10 m from the bend. The geometry was imported into ANSYS Workbench 2024 for CFD analysis. The use of an L-shaped design reflects realistic industrial layouts where directional changes occur before gas release. This setup allows a more practical evaluation of sensor performance in curved flow conditions.

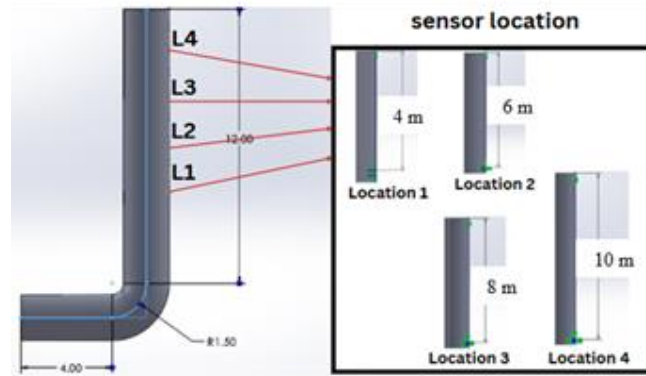


**Fig.1** L-shaped Stack Geometry Showing the Sensor Position

## 2.2 Meshing

The geometry was meshed using a standard patch conforming tetrahedral method with a 0.2 m element size, as shown in Fig. 2, to achieve a balanced resolution that captures essential flow features while minimizing computational cost. This mesh size was selected based on the grid independence test, which showed that the difference in average velocity between medium (0.2 m) and fine (0.1 m) mesh was less than 2%, indicating that further refinement would not significantly improve result accuracy. A coarse mesh (0.3 m) was also tested but showed higher deviation in predicted flow behavior. Therefore, the medium mesh was chosen for full-scale simulation as it offered sufficient detail, especially in the curved bend region, without excessive simulation time. Additionally, named selections were created for the inlet, outlet, and wall pipe to facilitate accurate assignment of boundary conditions during the simulation setup.

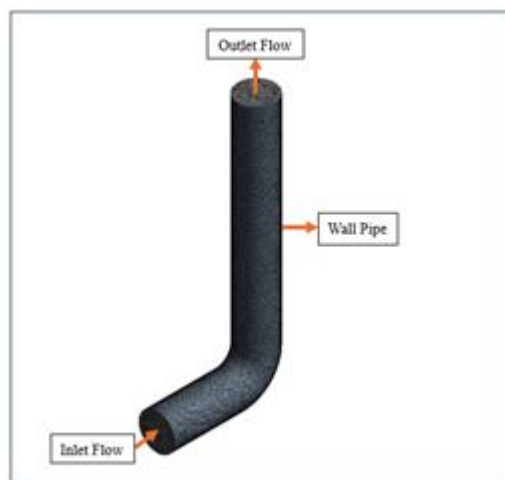


**Fig. 2** Mesh Structure of the Stack Model with Named Selection of Fluid Flow at Inlet, Outlet and Wall Pipe of Stack

## 2.3 Simulation Setup

A steady-state analysis was performed in ANSYS Fluent 2024 R1 to observe the fully developed flow behavior under constant conditions within the L-shaped flue gas stack. The flow was assumed to be incompressible, and gravity was applied in the negative Y-direction at  $-9.81 \text{ m/s}^2$  to replicate the natural downward flow effects. The working fluid was defined as a mixture of combustion by-products including carbon dioxide ( $\text{CO}_2$ ), nitrogen monoxide (NO), nitrogen dioxide ( $\text{NO}_2$ ), sulfur dioxide ( $\text{SO}_2$ ), carbon monoxide (CO), and oxygen ( $\text{O}_2$ ), which represent the common constituents in industrial flue gas. The inlet velocity was set at 10 m/s, the temperature at 323.15 K ( $50^\circ\text{C}$ ), and the turbulence intensity at 3.35%, based on referenced literature values relevant to flue gas emission studies. The outlet boundary condition was defined using gauge pressure set to 0 Pa to simulate atmospheric discharge. The standard  $k-\epsilon$  turbulence model was employed for its proven robustness and accuracy in simulating internal turbulent flows in industrial stack systems, particularly those involving bends and recirculation zones.

**Table 1** Parameter and Boundary Conditions

Parameter	Value
Simulation Type	Steady state
Solver	Pressure based
Gravity	Y-axis: -9.81 m/s
Inlet Velocity	10 m/s
Operating Temperature	323.15 K
Turbulence Flow Intensity, I	3.35%
Wall Condition	Adiabatic no-slip walls
Turbulence Model	Standard k- $\epsilon$
Working Fluids	CO <sub>2</sub> , CO, NO, NO <sub>2</sub> , SO <sub>2</sub> , O <sub>2</sub>

## 2.4 Solution Method

The solution method used second-order upwind schemes for momentum, energy, and turbulence equations to improve the accuracy of the simulation. A total of 200 iterations was set as the upper limit, although convergence was successfully achieved earlier at iteration 73, where all residuals fell below the standard threshold  $1 \times 10^{-3}$ . At the point of convergence, the continuity residual reached  $3.01 \times 10^{-4}$ , and turbulence variables (k and omega) were also within acceptable limits, indicating a stable and balanced flow field. The simulation did not require forced residual scaling or relaxation tuning, suggesting that the meshing and boundary condition setup were appropriately defined. In this study, the convergence was achieved smoothly, indicating that the simulation setup, including the mesh quality, inlet conditions, and solver settings, was effective. The residual plot in Fig. 3 illustrates the convergence behavior across iterations.

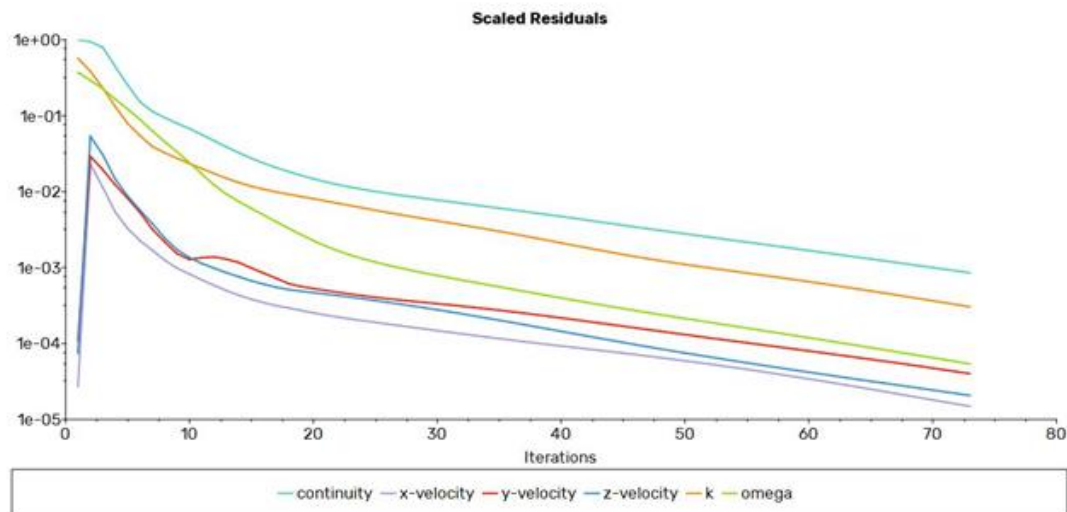


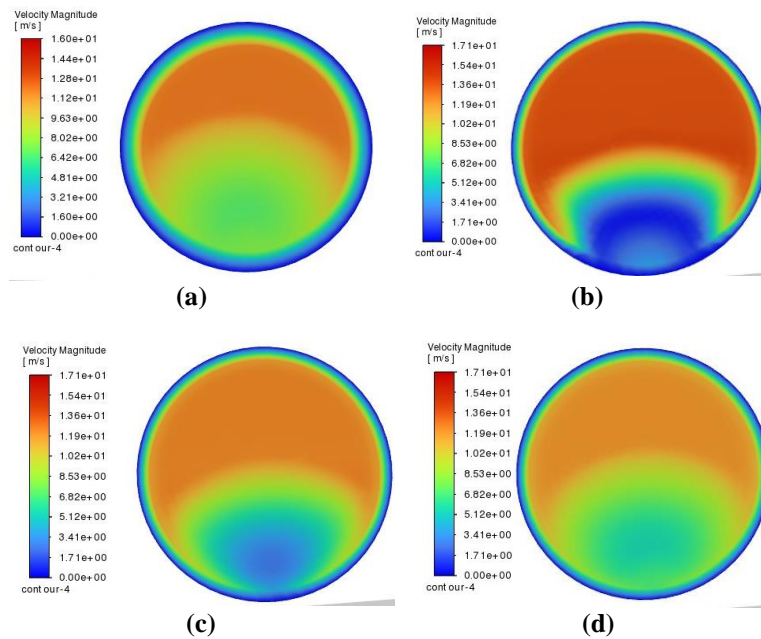
**Fig. 3** Residual Plot Showing Convergence of Continuity and Turbulence

## 3. Results and Discussion

### 3.1 Velocity Distribution

Velocity contours were analyzed to evaluate flow consistency at four different sensor locations along the vertical stack. At 4 meters from the bend at location 1, the flow exhibited the highest average velocity of 14.50 m/s, with strong velocity gradients and signs of turbulence, indicating that the flow was still developing. At 6 meters, which is Location 2, the velocity reduced to 12.75 m/s, and the streamlines became more organized, although some disturbance was still present. At 8 meters from the bend, which is at location 3, the flow showed an average velocity of 11.05 m/s, with smoother contours and reduced fluctuations. Finally, 10 meters from the

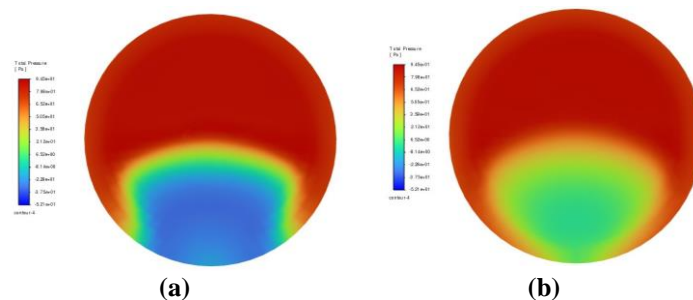
bend, which is location 4, the average velocity was 10.42 m/s, and the flow appeared fully developed and stable, with minimal directional change and uniform distribution. This gradual reduction in velocity and turbulence, as illustrated in Fig. 4, confirms that the farther the sensor is placed from the bend, the more stable and consistent the flow becomes, making location 4 the most suitable for accurate sensor placement.



**Fig. 4** Velocity Range with Color Gradient in Stack at Each Location (a) Location 1 (4 m) from Bend (b) Location 2 (6 m) from Bend (c) Location 3 (8 m) from Bend (d) Location 4 (10 m) from Bend

### 3.2 Pressure Distribution

Static pressure contours, as shown in Fig. 5, demonstrated a clear trend of increasing pressure uniformity further along the vertical stack. At 4 meters from the bend, which is at location 1, the pressure varied significantly, with a recorded pressure of 45.1 Pa, indicating uneven flow conditions and possible recirculation zones. At 6 meters at location 2, the pressure increased to 50.9 Pa, showing signs of stabilization. At 8 meters, which is location 3, the pressure was slightly higher at 51.0 Pa, with more consistent distribution across the sensor plane. Finally, at 10 meters at Location 4, the pressure reached 59.25 Pa, indicating the most stable and uniform pressure field among the four locations. This progression suggests that placing the sensor closer to the outlet allows it to operate in a more stable pressure environment, which is essential for improving the accuracy of pressure-sensitive measurement instruments.



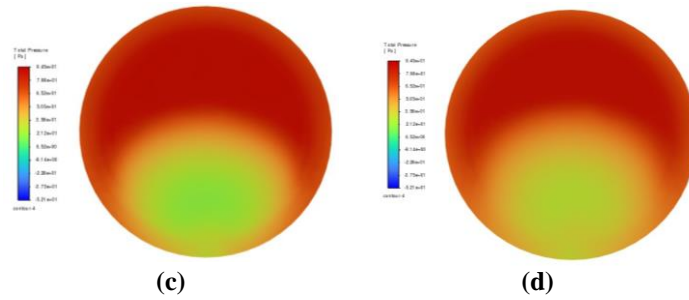


**Fig. 5** Pressure Range with Color Gradient in Stack at Each Locationr (a) Location 1 (4 m) from Bend (b) Location 2 (6 m) from Bend (c) Location 3 (8 m) from Bend (d) Location 4 (10 m) from Bend

### 3.3 Sensor Optimization and Comparative Analysis

To further analyze the suitability of each sensor location, a comparative assessment was conducted using two key parameters which are average velocity and pressure drop across the sensor. As presented in Fig. 6, the bar chart shows the average velocity at each proposed sensor location:

- Location 1, which is 4 meters from the bend, recorded the highest average velocity at 15.37 m/s, suggesting strong flow but potentially more turbulence and instability.
- Location 2, which is 6 meters from the bend, showed a slightly lower but still high velocity of 12.09 m/s, indicating moderate flow development.
- Location 3, which is 8 meters after the bend, had an average velocity of 14.58 m/s, which appears elevated, but might still present favorable flow behavior depend on pressure conditions.
- Location 4, which is 10 meters from the bend or 2 meters before the outlet, recorded the lowest average velocity at 11.56 m/s, indicating a more settled and fully developed flow profile.

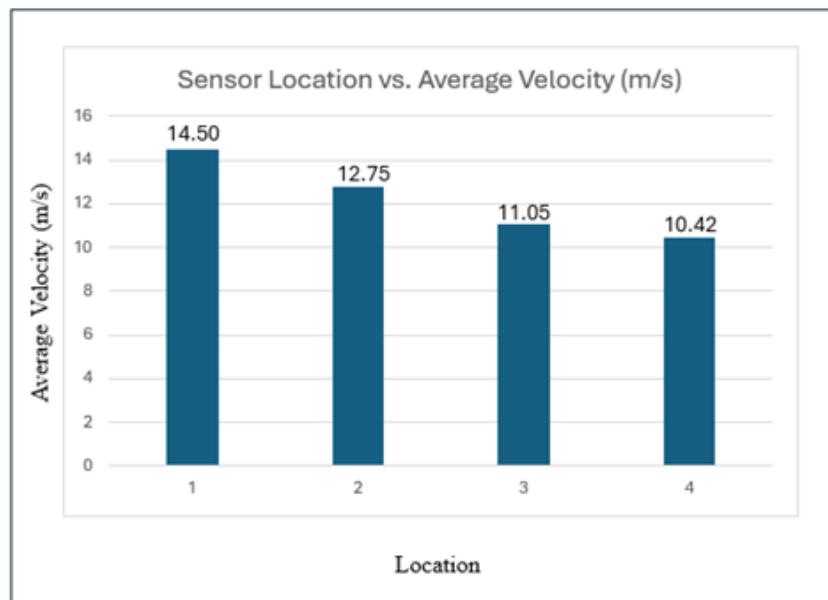


**Fig. 6** Comparison of Average Velocity at Each Location

Fig. 7 illustrates the average pressure recorded at four different sensor locations along the vertical stack. As shown in the chart, location 1 (4 meters from the bend) recorded the lowest average pressure of 28.50 Pa, indicating the presence of more turbulent and unstable flow, typically found closer to the flow transition zone after the bend. As the sensor placement moves further up the stack, the average pressure increases gradually, reflecting more stabilized flow conditions. Location 2 (6 meters from the bend) and location 3 (8 meters from the bend) show similar average pressures of 42.65 Pa and 43.15 Pa, respectively, suggesting moderate stability and uniformity in the pressure field. The highest average pressure was observed at location 4 (10 meters from the bend or 2 meters before the outlet), reaching 57.85 Pa. This increase indicates a fully developed flow region

with consistent pressure distribution, making it the most favorable zone for sensor placement. The overall trend supports the fact that as the gas travels upward through the vertical stack, the flow becomes more uniform, and pressure conditions stabilize, which is critical for ensuring accurate and reliable sensor readings.

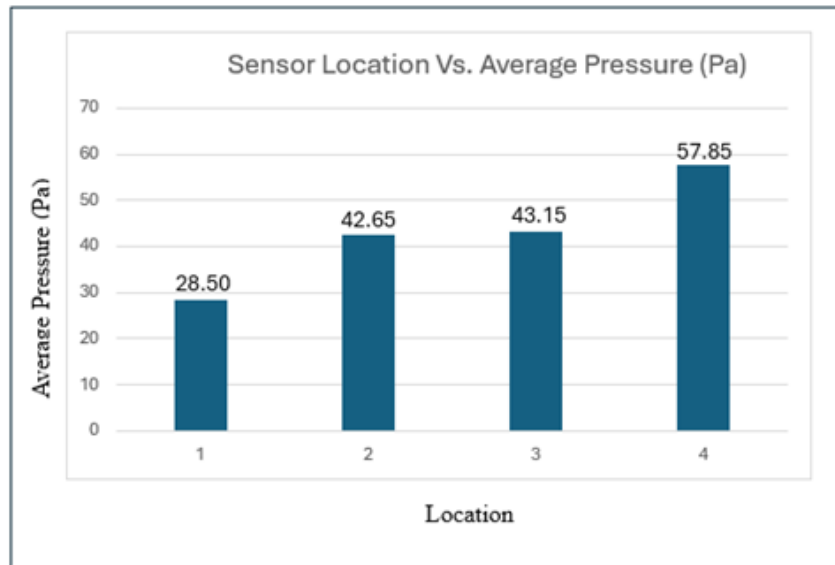


Fig. 7 Comparison of Average Pressure at Each Location

### 3.4 Recommended Sensor Placement

Fig. 8 displays the streamline visualization of flue gas flow within the L-shaped stack and highlights the four proposed sensor locations positioned at 4 m, 6 m, 8 m, and 10 m above the bend. The streamline patterns illustrate how the gas flow evolves as it travels vertically upwards. At location 1 (4 m from bend), the streamlines are more curved and irregular due to the influence of the bend, indicating areas of disturbance and incomplete flow development. As the flow continues upward to location 2 (6 m from bend) and location 3 (8 m from bend), the streamlines become smoother and more aligned with the pipe wall, reflecting increasingly stabilized flow behavior. The most uniform and fully developed flow is observed at location 4 (10 m from bend), where the streamlines show minimal curvature or separation, suggesting optimal conditions for sensor installation. This region experiences reduced turbulence and more consistent flow, which is essential for improving the accuracy of in-situ gas monitoring. As marked in the figure, location 4 is identified as the best location for sensor placement due to its balanced flow characteristics and minimal disruption, confirming the simulation's findings.

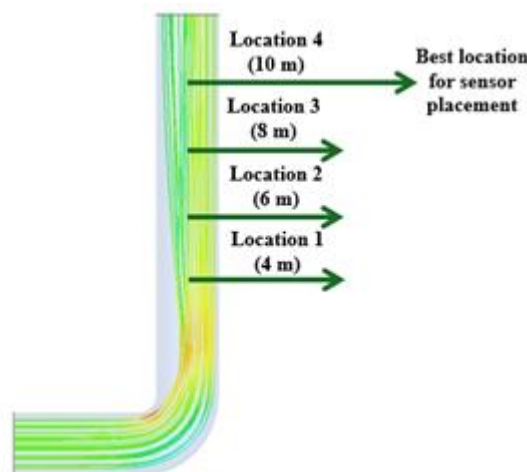


Fig. 8 Best Sensor Location in L-shaped Stack

## 4. Conclusion

This study successfully employed Computational Fluid Dynamics (CFD) to investigate the flue gas flow behavior within an L-shaped industrial exhaust stack and to identify the optimal location for in-situ sensor placement for emission monitoring. Through simulation using ANSYS Fluent, it was found that the gas flow becomes progressively more stable as it travels further from the stack bend. Among the four evaluated positions, Location 4, which is 10 meters from the bend or 2 meters before the outlet, demonstrated the most favorable conditions, with an average velocity of 10.42 m/s and a small pressure difference of 2.42%, indicating fully developed flow and minimal turbulence or interference around the sensor probe.

These results underscore the importance of proper sensor positioning to ensure accurate and reliable data collection in real-time monitoring systems. Accurate placement not only minimizes measurement errors but also enhances the detection of harmful pollutants such as CO<sub>2</sub>, NO<sub>x</sub>, and SO<sub>2</sub>, which are critical to air quality management. The use of CFD provides a cost-effective and efficient alternative to experimental methods, enabling industries to optimize sensor deployment while reducing development time and resources.

Moreover, the outcomes of this study support broader environmental and regulatory efforts. By improving the precision of emission monitoring, this work aligns with key objectives of the Sustainable Development Goals (SDGs), particularly SDG 13 (Climate Action) and SDG 12 (Responsible Consumption and Production). For future work, it is recommended to extend the analysis by incorporating thermal effects, gas species behavior, and validation with experimental or field data. The methodology demonstrated here serves as a robust foundation for advancing sensor placement strategies in industrial emission systems, promoting smarter, cleaner, and more sustainable engineering solutions.

## Acknowledgement

Communication of this research is made possible through monetary assistance by Universiti Tun Hussein Onn Malaysia, and this research was also supported by Universiti Tun Hussein Onn Malaysia (UTHM) Research Management Center (RMC) provided through the GPPS (vot J053).

## Conflict of Interest

The authors declare that there is no conflict of interest regarding the publication of the paper.

## Author Contribution

*All authors confirm their contribution to the paper as follows: **study conception and design, data collection analysis and interpretation of results and draft manuscript preparation.** All authors reviewed the results and approved the final version of the manuscript.*

## References

- [1] AZIZI, M., & Hashim, N. H.. (2021). Wind Rose Analysis for UTHM and Possible Pollution Sources Zone. *Progress in Engineering Application and Technology*, 2(1), 432-443. <https://publisher.uthm.edu.my/periodicals/index.php/peat/article/view/1066>
- [2] M. A. Elseoud, A. A. El-Rahman, and H. Saleh, "Modeling of a Thermoacoustic Flue Gas Analyzer," *J Thermophys Heat Trans*, pp. 1-9, Sep. 2024, doi: 10.2514/1.T7027
- [3] M. N. Bin Nawawi, H. Bin Samsudin, J. Saputra, K. Szczepańska-Woszczyna, and S. Kot, "The Effect of Formal and Informal Regulations on Industrial Effluents and Firm Compliance Behavior in Malaysia," *Production Engineering Archives*, vol. 28, no. 2, pp. 193-200, Jun. 2022, doi: 10.30657/pea.2022.28.23.
- [4] "Environmental Quality (Clean Air) Regulation 2014".
- [5] A. Sarwar, S. M. F. Azam, N. Khan, M. Raman, V. O. K. Seng, and A. Siddika, "Critical Factors Impacting the Implementation of Environmental Protection Strategies among Malaysia Industries," *International Journal of Energy Economics and Policy*, vol. 13, no. 1, pp. 431-442, 2023, doi: 10.32479/ijeep.13279.
- [6] A. N. Johnson et al., "Faster, more accurate, stack-flow measurements," *J Air Waste Manage Assoc*, vol. 70, no. 3, pp. 283-291, Mar. 2020, doi: 10.1080/10962247.2020.1713249.
- [7] M. Shen, L. Tong, H. Ding, L. Wang, and Y. Ding, "Numerical investigation of flow stratification behavior of binary particle mixture for high-temperature flue gas filtration on an inclined moving bed," *Powder Technol*, vol. 382, pp. 339-350, Apr. 2021, doi: 10.1016/j.powtec.2020.12.059.
- [8] S. Guo et al., "A multi-laser hybrid absorption sensor for simultaneous measurement of NH<sub>3</sub>, NO, and temperature in denitrification flue gas," *Infrared Phys Technol*, vol. 136, Jan. 2024, doi: 10.1016/j.infrared.2023.105034.

- [9] T. R. Andersson et al., "Environmental sensor placement with convolutional Gaussian neural processes," *Environmental Data Science*, vol. 2, 2023, doi: 10.1017/eds.2023.22.
- [10] M. Farid and D. Solav, "Data-driven sensor placement optimization for accurate and early prediction of stochastic complex systems," *J Sound Vib*, vol. 543, Jan. 2023, doi: 10.1016/j.jsv.2022.117317.
- [11] H. Cao, Y. Yu, P. Zhang, and Y. Wang, "Flue gas monitoring system with empirically-trained dictionary," *IEEE/CAA Journal of Automatica Sinica*, vol. 7, no. 2, pp. 606–616, Mar. 2020, doi: 10.1109/JAS.2019.1911642.
- [12] M. G. V. D, B. N., and B. H. B. A., "Comparative Investigations and CFD Analysis of Flue Gas Flow through Novel Kitchen Chimney Design," Oct. 24, 2022. doi: 10.21203/rs.3.rs-2179779/v1.
- [13] Jumadi, R., Khalid, A., Jaat, N., Abdullah, I. S., Darlis, N., Manshoor, B., Razali, A., Sapit, A., & Nursal, R. S. (2020). Analysis of Spray Characteristics and High Ambient Pressure in Gasoline Direct Injection using Computational Fluid Dynamics. *CFD Letters*, 12(5), 36–51. <https://doi.org/10.37934/cfdl.12.5.3651>
- [14] Razali, M. A., Mohideen Batcha, M. F. ., Madon, R. H. ., Khalid, A. ., Mohmad Ja'at, M. N. ., Sapit, A. ., Mohammed, A. N. ., Mat Zaki, M. A. ., & Samsubaha, M. F. . (2020). Development of Experimental Apparatus to Analyze Diesel Spray Characteristics. *International Journal of Integrated Engineering*, 12(3), 14-21. <https://publisher.uthm.edu.my/ojs/index.php/ijie/article/view/2738>
- [15] Azwan Sapit, Mohd Azahari Razali, Mohd Faisal Hushim, Amir Khalid, Md Norrizam Mohmad Ja'at, Muhammad Fauzi Samsubaha, & Tuan Mohamad Kamarul Hisyam Tuan A Talib. (2024). Effect of Acoustic Excitation toward Jet Flame: An Experimental Design. *Journal of Advanced Research in Fluid Mechanics and Thermal Sciences*, 53(1), 69–74. Retrieved from [https://semarakilmu.com.my/journals/index.php/fluid\\_mechanics\\_thermal\\_sciences/article/view/3002](https://semarakilmu.com.my/journals/index.php/fluid_mechanics_thermal_sciences/article/view/3002)
- [16] Hashim, A., Khalid, A., Jaat, N., Sapit, A., Razali, A., & Nizam, A. (2017). Analysis of high injection pressure and ambient temperature on biodiesel spray characteristics using computational fluid dynamics. *IOP Conference Series: Materials Science and Engineering*, 243, 012049. <https://doi.org/10.1088/1757-899x/243/1/012049>
- [17] Tukiman, M. M., Ghazali, M. N. M., Sadikin, A., Nasir, N. F., Nordin, N., Sapit, A., & Razali, M. A. (2017). CFD simulation of flow through an orifice plate. *IOP Conference Series: Materials Science and Engineering*, 243, 012036. <https://doi.org/10.1088/1757-899x/243/1/012036>
- [18] Sapit, A., Razali, M. A., Hushim, M. F., Jaat, N., Mohammad, A. N., & Khalid, A. (2017). Comparison on dynamic behavior of diesel spray and rapeseed oil spray in diesel engine. *Journal of Physics: Conference Series*, 822, 012058. <https://doi.org/10.1088/1742-6596/822/1/012058>
- [19] Khalid, A., Jaat, N., Hushim, M. F., Manshoor, B., Zaman, I., Sapit, A., & Razali, A. (2017). Computational Fluid Dynamics Analysis of High Injection Pressure Blended Biodiesel. *IOP Conference Series: Materials Science and Engineering*, 226, 012002. <https://doi.org/10.1088/1757-899x/226/1/012002>
- [20] Samsubaha, M. F., Razali, M. A., Madon, R. H., Khalid, A., Mohmad Ja'at, M. N., Manshoor, B., Sapit, A., Muhammad, A. N., & Salleh, H. (2020). Acoustic Perturbation Toward Jet Flame – Variation of Flame Shapes Mode. *Journal of Advanced Research in Fluid Mechanics and Thermal Sciences*, 73(1), 140–145. <https://doi.org/10.37934/arfmts.73.1.140145>